NANO LETTERS

Letter

pubs.acs.org/NanoLett

Visible Light Driven Photoelectrochemical Water Oxidation on Nitrogen-Modified TiO_2 Nanowires

Son Hoang,[†] Siwei Guo,[†] Nathan T. Hahn,[†] Allen J. Bard,[‡] and C. Buddie Mullins*[,†,‡]

[†]Department of Chemical Engineering, [‡]Department of Chemistry and Biochemistry, Center for Electrochemistry, Texas Materials Institute, Center for Nano and Molecular Science, University of Texas at Austin, 1 University Station C0400 Austin, Texas 78712-0231, United States

Supporting Information

ABSTRACT: We report hydrothermal synthesis of single crystalline TiO_2 nanowire arrays with unprecedented small feature sizes of ~5 nm and lengths up to 4.4 μm on fluorine-doped tin oxide substrates. A substantial amount of nitrogen (up to 1.08 atomic %) can be incorporated into the TiO_2 lattice via nitridation in NH_3 flow at a relatively low temperature (500 °C) because of the small cross-section of the nanowires. The low-energy threshold of the incident photon to current efficiency (IPCE) spectra of N-modified TiO_2 samples is at ~520 nm, corresponding to 2.4 eV. We also report a simple cobalt treatment for improving the photoelectrochemical (PEC) performance of our N-modified TiO_2 nanowire arrays. With the cobalt treatment, the IPCE of N-modified TiO_2 samples in the ultraviolet region is restored to equal or higher values than those of the unmodified TiO_2 samples, and it remains as high as ~18% at 450 nm. We propose that the cobalt treatment enhances PEC performance via two mechanisms: passivating surface states on the N-modified TiO_2 surface and acting as a water oxidation cocatalyst.

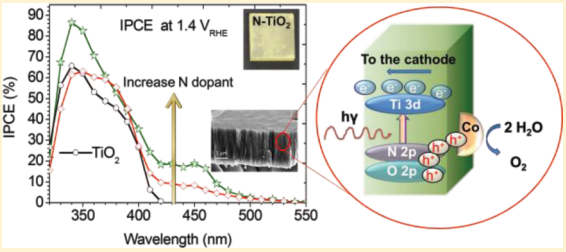

KEYWORDS: *Water photo-oxidation, N-modified TiO_2, water oxidation catalyst, hydrothermal synthesis, single crystalline nanowire, photocatalysis*

Titanium dioxide (TiO_2) is well-known as a candidate for water photo-oxidation as it is abundant, stable in aqueous solution under irradiation, and has strong photocatalytic activity.[1,2] However, due to its large band gap (~3.0 eV for rutile and 3.2 eV for anatase), TiO_2 is only active in the ultraviolet (UV) region which contributes less than 5% of the total energy of the solar spectrum.[3] Shifting the absorption of TiO_2 to include visible light, which composes a greater portion of the solar spectrum (45%), is one of the prerequisites to enhancing the solar energy conversion efficiency of titania.[4−7] Another requirement of an effective photomaterial is good electron−hole separation characteristics, which can be improved by increasing the charge transfer (normally via nanostructuring the morphology and doping with foreign ions) and increasing the kinetics of water oxidation by holes and water reduction by electrons (via loading of cocatalysts). TiO_2 has a short hole diffusion length (~10 nm for the rutile single crystal),[8] therefore it is necessary to reduce the TiO_2 characteristic size to decrease the diffusion pathway of photoholes to the electrode/electrolyte interface. Moreover, in a photoelectrochemical (PEC) cell, electrons generated in the TiO_2 photoanode film have to travel within the TiO_2 film to the back contact and then transfer to the cathode. Therefore the optimum morphology is a one-dimensional, single crystalline structure to enable electrons to travel to the back contact and holes to diffuse to the electrode/electrolyte interface in the easiest manner without scattering at a grain boundary. Co-catalysts, such as IrO_2,[9] Co-based materials,[10] and Co-Pi[11] for water oxidation, are also needed to increase the kinetics of the reactions, thus reducing the charge recombination rate.

Incorporating nitrogen has been said to narrow the band gap of TiO_2 for water splitting applications since substitutional N 2p states hybridize with O 2p states, upshifting the valence band edge while almost keeping the conduction band edge in the same position.[4,12,13] However, there is an ongoing debate regarding the red shift of the absorption edge of N-modified TiO_2. Some researchers believe substitutional N forms isolated N 2p midgap states slightly above the top of the O 2p valence, instead of mixing with O 2p to form a continuous valence band as proposed above.[14−16] In this case, photogenerated holes may be trapped in these localized states leading to a high recombination rate, thus decreasing the quantum yields of N-modified TiO_2. Some other researchers suggest that high doping of nitrogen in TiO_2 produces color centers with a different local chemical composition and electronic structure.[17,18] In this picture, the color centers, including Ti^{3+}, are responsible for visible light absorption in the N-modified TiO_2 material.

Received: August 15, 2011
Revised: November 3, 2011
Published: November 23, 2011

Nitrogen incorporation can be accomplished by calcining TiO_2 under NH_3. However, due to the low solubility of N in the TiO_2 lattice, the reactions normally have to be conducted at high temperatures (above 550 °C) to yield sufficient N-dopant incorporation for better visible light absorption. However, annealing in NH_3 at such high temperatures leads to unwanted side effects, such as defect formation within the TiO_2 lattice, degradation of the transparent conductive substrate [fluorine-doped tin oxide (FTO)], and sintering of the nanostructure.

In this Letter, we report a simple hydrothermal synthesis route for growing densely packed, vertical, single crystalline TiO_2 rutile nanowire arrays on FTO substrates of unprecedented small cross-sections with a characteristic dimension of ~5 nm and lengths up to 4.4 μm. A significant amount of nitrogen (up to 1.08 atomic %) can be incorporated into the TiO_2 by annealing the films under NH_3 flow at a relatively low temperature (500 °C) because of the exceptionally small nanowire cross-section. Furthermore, we report a simple surface treatment employing cobalt as a cocatalyst that we believe has not been investigated previously with TiO_2, in order to improve the water oxidation performance of N-modified TiO_2. N-modified TiO_2 films without a cobalt cocatalyst yielded a lower photocurrent under a full spectrum and lower quantum yields in the UV region than similar unmodified TiO_2 samples, although the N-modified samples had higher visible light photocurrents. A cobalt cocatalyst not only enhances the quantum yield in the visible light region but also restores the quantum yield in the UV region compared to the equivalent values of the unmodified samples.

Synthesis of TiO_2 Nanowire Arrays. FTO-coated glass substrates were first cleaned by sonication in a mixture of ethanol and water for 30 min, subsequently rinsed with deionized (DI) water, and finally dried in an air stream. In order to enhance the sample integrity and shorten the growing time, FTO substrates were also seeded with a thin layer of TiO_2 before growing the nanowire arrays. For seeding, clean FTO substrates were first soaked in 0.025 M $TiCl_4$ in *n*-hexane for 30 min. They were then taken out, rinsed by ethanol, and finally annealed in air at 500 °C for 30 min. In a typical hydrothermal growth procedure, the seeded FTO substrates were placed on the bottom of a Teflon-lined autoclave (125 mL, Parr Instrument), containing 50 mL of *n*-hexane (extra dry, 96+%, Acros Organics), 5 mL of HCl (ACS reagent grade 36.5−38%, MP), and 2.5−5 mL of titanium(IV) isopropoxide (98+%, Acros Organics). The hydrothermal synthesis was conducted at 150 ° C for certain amount of time in a box oven. After the reaction was completed and the autoclave naturally cooled down to room temperature, the TiO_2 nanowire films were taken out and cleaned by rinsing with copious amount of ethanol and water.

The hydrothermal growth of vertical TiO_2 nanowire arrays on FTO with feature sizes of ~20 nm via a nonpolar solvent/hydrophilic solid substrate interfacial reaction was first reported by Grimes and co-workers.[19] Using a similar strategy, we developed the recipe (i.e., titanium precursors, nonpolar solvents) and the hydrothermal reaction conditions (i.e., reaction time and temperature) described above that enable the synthesis of high-quality rutile TiO_2 single crystalline nanowire arrays with smaller feature sizes (~5 nm). As proposed by Grimes et al.,[19] at room temperature, titanium precursors [e.g., titanium tetraisopropoxide (TTIP)] and water (from hydrochloric acid solution) are separated since the precursors are soluble and water is immiscible in the nonpolar solvents (e.g., *n*-hexane). Under hydrothermal conditions, to minimize system energy, water diffuses to the hydrophilic FTO surface where it hydrolyzes with TTIP to form TiO_2 nuclei on the FTO surface. As the newly formed TiO_2 nuclei are also hydrophilic, water continues to diffuse to the nuclei resulting in further hydrolysis and crystal growth. The Cl^- ions play an important role in the hydrothermal growth as they promote anisotropic growth of one-dimensional nanocrystals. The Cl^- ions are inclined to absorb on the rutile (110) plane, thus retarding further growth of this plane. We did not observe nanowire array formations when HCl was replaced by HNO_3 or H_2SO_4.

Characterization of TiO_2 Arrays. Shown in Figure 1a,b are cross-sectional and top view scanning electron microscope (SEM) images of a typical as-synthesized (with no further heat treatment) nanowire film. The nanowire arrays consisting of vertically aligned and tetragonal shaped nanowires are highly uniform and densely packed with exceptionally small feature sizes (average characteristic cross-sectional dimension is ~5 nm). The grazing incidence X-ray diffraction (GIXRD) pattern in Figure 1d shows that the as-synthesized nanowire arrays are rutile TiO_2 with an enhancement in the (101) facet exposure relative to the standard rutile powder pattern (JCPDS #88-1175). The high-resolution transmission electron microscope (HRTEM) image in Figure 1c further confirms that the nanowires are single crystalline with an interplanar *d*-spacing of 0.327 nm, corresponding to (110) planes of rutile TiO_2. The atomic ratio of Ti to O was found to be ~1:2 using energy dispersive X-ray analysis (EDX) (the expected stoichiometric values).

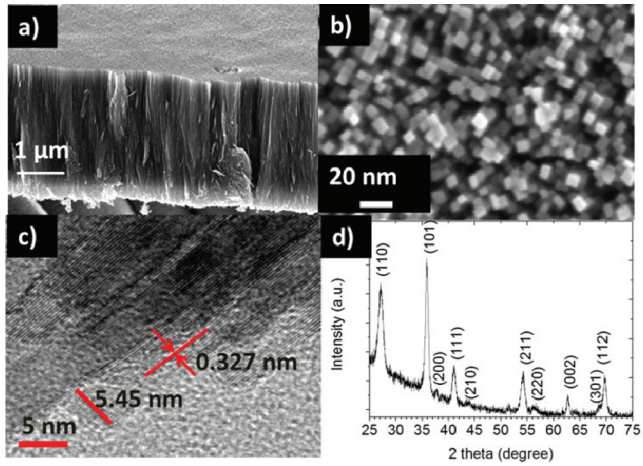

Figure 1. Vertically aligned single crystalline TiO_2 rutile nanowire arrays on FTO glass: (a) cross-sectional and (b) top view SEM images, (c) HRTEM image, and (d) grazing incidence angle X-ray diffraction (GIXRD) pattern.

The length of the nanowire arrays is a function of the TTIP to *n*-hexane volume ratio, the reaction conditions (i.e., temperature and time), and seeding layer. The thicknesses of nanowire arrays versus reaction conditions, determined from cross-sectional view SEM, are shown in Table 1. We are able to grow nanowires with lengths varying from ~500 nm up to 4.4 μm with no significant change in feature sizes. Moreover, if the FTO substrates are coated with a thick TiO_2 layer (~5 μm) prior to hydrothermal reaction, we can grow nanowire arrays with lengths up to 17 μm. Optimization of the thickness of a

dx.doi.org/10.1021/nl2028188 | *Nano Lett.* 2012, 12, 26−32

Table 1. Thicknesses of Some TiO_2 Nanowire Arrays Grown at 150 °C As a Function of TTIP/n-Hexane Ratio, Reaction Time, and Seeding Layer

TTIP/*n*-hexane volume ratio	reaction time (hour)	seeding	number of sample(s)	length of nanowires
1:20	5	no	1	500 nm
1:20	5	yes	20	1.59 ± 0.26 μm
1:10	5	no	4	1.2 ± 0.26 μm
1:10	5	yes	22	2.6 ± 0.27 μm
1:10	10	yes	4	4.4 ± 0.27 μm

photoelectrode for PEC applications involves balancing the charge carrier mobility and the absorbance of photons. The photoanode should be as thin as possible to allow electrons to travel to the back contact in the shortest time while still being thick enough to absorb the majority of the photons from sunlight. In our study, the highest photocurrents were from samples with thicknesses of ~1.5 μm. Therefore, we focused on the PEC characterization of TiO_2 nanowire films with thicknesses of 1.59 ± 0.26 μm grown at 150 °C for 5 h with TTIP/*n*-hexane ratios of 1:20.

The seeding layer enhances both the nanowire arrays' adherence to the FTO substrate and the growth rate. For example, the thickness of TiO_2 nanowire arrays grown with the ratio TTIP/*n*-hexane of 1/10 at 150 ° C for 5 h with and without the seeding layer is 2.60 ± 0.27 and 1.2 ± 0.15 μm, respectively. As mentioned above, when FTO was coated with a thick TiO_2 seeding layer of ~5 μm, the same reaction conditions resulted in a nanowire length of ~17 μm.

We found that the combination of titanium precursor and nonpolar solvent strongly affects the morphology of the nanowire arrays. Using a combination of titanium(IV) tetra-*n*-butoxide (TNBT) (Ti^{4+} precursor) and *n*-hexane or a combination of TTIP and toluene (nonpolar solvent) resulted in unoriented, wire bundle formation. We further investigated nanowire array growth using a combination of TNBT and toluene which resulted in oriented but shorter nanowire arrays (~1.3 μm) with bigger feature sizes (~15 nm) (Figure S1, Supporting Information).

PEC Properties of TiO_2 Nanowire Arrays. The PEC characterization of TiO_2 nanowire samples was performed using a three-electrode electrochemical cell with the FTO supported nanowire arrays as the working electrode, a Ag/AgCl (saturated KCl) reference electrode, a platinum wire counter electrode, and 1 M KOH electrolyte (pH = 13.5). The working electrode with exposed area of 0.16 cm^2 was illuminated from the back side (through the FTO substrate−TiO_2 nanowire interface) by a 100 W xenon lamp (Newport) through a UV/IR filter (Schott, KG3) to remove infrared (>800 nm) and short wavelength UV light (<300 nm). Using a Scientech calorimeter (model 38-0101), the light intensity of the spectrum from 400 nm to 1.2 μm was measured as 37 mW/cm^2. The fraction of the total energy of the spectrum from 400 to 800 nm for our lamp is estimated to be 85−90% of the total light energy, therefore, we estimate the energy flux in our PEC measurements to be ~41−43 mW/cm^2. Incident photon to current conversion efficiencies (IPCEs) were calculated from amperometry measurements using a monochromator (Newport) with a bandwidth of 7.4 nm in conjunction with a power meter and photodiode (Newport), given by

$$\mathrm{IPCE} = \frac{1240 \times j_{\mathrm{ph}}}{\lambda \times I} \times 100\% \quad (1)$$

where j_{ph} is the steady-state photocurrent density at a specific wavelength, and λ is the wavelength of the incident light. I is the light intensity for wavelength λ at the film surface, I ranges from 80 to 300 μW/cm^2 over the spectrum of wavelengths studied (320−550 nm).

The measured potentials versus the Ag/AgCl reference electrode were converted to the reversible hydrogen electrode (RHE) scale via the Nernst equation:

$$E_{\mathrm{RHE}} = E_{\mathrm{Ag/AgCl}} + 0.059\ \mathrm{pH} + E^{\circ}_{\mathrm{Ag/AgCl}} \quad (2)$$

where E_{RHE} is the converted potential vs RHE, $E_{Ag/AgCl}$ is the experimental potential measured against the Ag/AgCl reference electrode, and $E^{\circ}_{Ag/AgCl}$ is the standard potential of Ag/AgCl at 25 °C (0.1976 V). We also used the same testing conditions for other samples throughout this paper.

Before testing, the as-synthesized films were annealed in air at 500 °C for 1 h to remove contaminants and increase the adherence of the TiO_2 arrays to the SnO_2 layer. Figure 2a shows the linear sweep voltammetry of the TiO_2 nanowire sample. The onset potential of our TiO_2 nanowire arrays is ~0.2 V_{RHE}, around 0.2 V more negative compared to a TiO_2 nanotube sample.[5] In order to improve the PEC performance, we also applied a cobalt treatment technique similar to that reported by Grätzel et al.[10] in which the TiO_2 nanowire arrays were soaked in 0.1 M $Co(NO_3)_2$ for 1 min, followed by rinsing

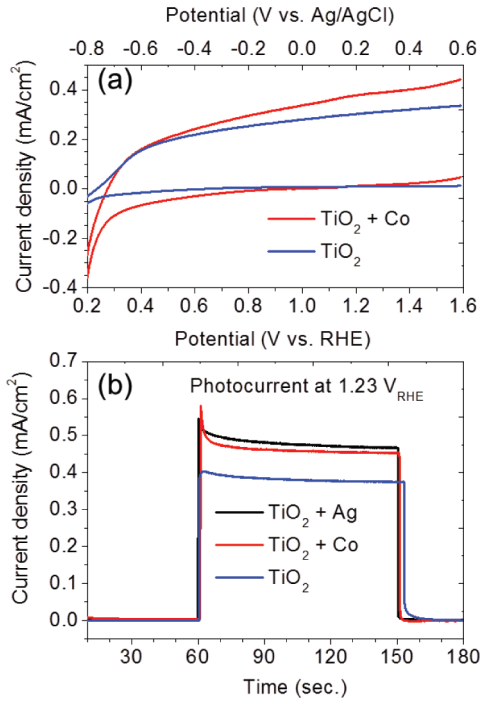

Figure 2. (a) Linear sweep voltammetry measurements of TiO_2 nanowire arrays (1.6 μm) and the same film after cobalt treatment and (b) chronoamperometry measurement (at 1.23 V_{RHE}) of TiO_2 nanowire arrays and the same film after cobalt and silver treatments (cobalt and silver treatments were performed on two different areas on the same TiO_2 nanowire sample). All experiments were performed with 1 M KOH electrolyte (pH = 13.5) and a 100 W xenon lamp coupled with a UV/IR filter as the light source as described in the text.

dx.doi.org/10.1021/nl2028188 | *Nano Lett.* 2012, 12, 26−32

with a copious amount of water. The photocurrent measured at 1.23 V_{RHE} was improved by ~20% due to the cobalt treatment, from 0.38 mA/cm^2 (without treatment) to 0.46 mA/cm^2. Cobalt-based materials, such as Co-Pi, are well-known catalysts for the water oxidation reaction.[11] However, to our knowledge, there have not been any reports on PEC enhancement of TiO_2 due to loading cobalt as a cocatalyst, probably due to the high intrinsic oxidative power of the holes photogenerated within the valence band of TiO_2. We speculate that in this case the cobalt treatment improves the PEC performance mainly via the saturation of dangling bonds on the TiO_2 surface, thus passivating the surface states which act as charge recombination centers. Employing a silver treatment (similar to cobalt treatment), in which 0.05 M $AgNO_3$ replaced 0.1 M $Co(NO_3)_2$, leads to a similar improvement (Figure 2b), supporting our speculation.

We have also noticed that the orientation of the FTO placed in the reactor, i.e., whether it 'faces up' or 'faces down' during the nanowire growth affects the PEC performance, although it does not affect the growth rate of the nanowire arrays. The films grown with the FTO 'facing up' yielded a photocurrent ~10−15% higher than films grown with the FTO 'facing down'. The samples grown with the FTO 'facing up' have some flower-like microsize particles on top (Figure S2, Supporting Information) which have been reported to enhance light harvesting, thus improving the PEC performance.[20,21]

Synthesis of N-Modified TiO_2 Nanowire Arrays. Nitrogen-modified TiO_2 films were prepared by annealing TiO_2 nanowire films in an NH_3 flow (100 mL/min) at temperatures from 400 to 650 °C. The color of all films changed from cloudy white to bright yellow, indicating successful N incorporation. The average feature size of N-modified TiO_2 nanowires is around 15 nm, larger than that of the as-synthesized sample, probably due to sintering of the nanowires at elevated temperatures (Figure S3, Supporting Information). At calcination temperatures higher than 500 °C (i.e., 550, 600, and 650 °C), FTO substrates were damaged and not electrically conductive. Wang et al. reported that at temperatures higher than 550 °C, NH_3 decomposes, releasing H_2 and causing partial reduction of TiO_2.[22] The appearance of Sn signals in the XRD patterns of these films suggests that the SnO_2 layer was also reduced (data not shown). Compared with films annealed at lower temperatures (i.e., 400 and 450 °C), films nitrided at 500 °C showed the highest photocurrent. Therefore, we focused on characterizing films annealed in NH_3 at 500 °C.

Chemical Characterization of N-Modified TiO_2 Nanowire Arrays. The N 1s XPS spectra of TiO_2 nanowire films annealed at 500 °C in NH_3 flow both for 1 and 2 h are shown in Figure 3a,3 and 4, respectively. Two N 1 s binding energy peaks around 400 and 394 eV in the films annealed in NH_3 clearly indicate that N has been successfully incorporated into the TiO_2 lattice. The N 1s peak at ~400 eV can be attributed to either interstitial N[23,24] atoms or chemisorbed N-containing gas, such as NH_3 or N_2.[4,25,26] However, its origin and contribution to visible light absorption are still under debate. According to early XPS investigations on N-modified TiO_2,[12,22,24−26] the N 1s peak at 392−396 eV was assigned to β−N in the Ti−N bond or N substituted at oxygen sites (substitutional N). There is no TiN formation indicated in the XRD and also no Ti^{3+} in the XPS spectra (a typical one is shown in Figure 3b,2) of these films, suggesting that the N 1s peak at 394 eV in our N-modified TiO_2 samples may be

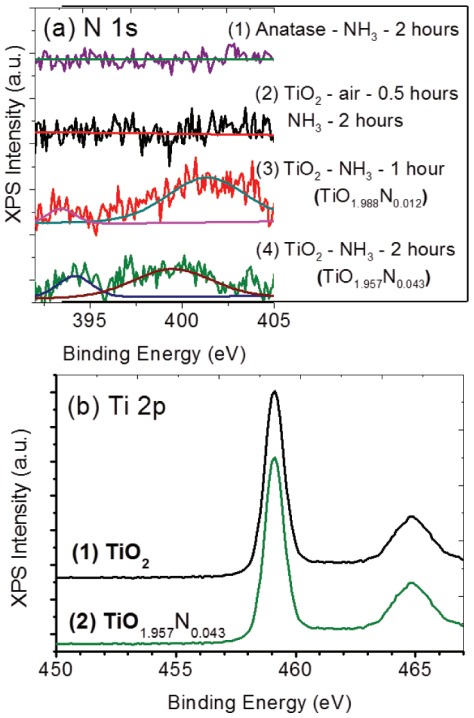

Figure 3. (a) Core N 1s XPS spectra of (1) anatase powder annealed in NH_3 for two hours, (2) TiO_2 nanowire film annealed in air for 30 min and then annealed in NH_3 for two hours, and (3) and (4) TiO_2 nanowire films annealed in NH_3 at 500 °C for 1 and 2 h, respectively. (b) Core Ti 2p XPS spectra of (1) as-synthesized TiO_2 nanowire film and (2) a TiO_2 nanowire film annealed in NH_3 at 500 °C for 2 h.

assigned as substitutional N, resulting in a composition that can be described as $TiO_{2-x}N_x$. The substitutional N species is commonly recognized as a contributor to visible light absorption and changes in photocatalytic activity. For example, Irie et al.[25] reported a monotonic increase in visible light absorption, yet a monotonic decrease in photocatalytic activity with an increase in the substitutional N concentration. In addition, we did not observe formation of Ti^{3+} (Figure 3b), one of the most important types of color centers. Therefore we believe that the substitutional N species found at 394 eV is likely the main contributor to visible light absorption and changes in the water photo-oxidation performance in the TiO_2 nanowire films, as shown in the next section.

Shown in Table 2 is our XPS analysis with atomic percentages of substitutional N in films annealed for 1 and 2

Table 2. N-Dopant Concentration in TiO_2 Nanowire Films Annealed at 500 °C in NH_3

annealing conditions	N content/peak position (atomic %, eV)	x in $TiO_{2-x}N_x$
500 °C, NH_3, 1 h	0.35%, 393.4 eV 3.41%, 401.3 eV	0.012
500 °C, NH_3, 2 h	1.08%, 394.2 eV 3.04%, 399.3 eV	0.043

h of 0.35 and 1.08%, respectively. Since the surface is rich in oxygen, probably due to the adsorption of oxygen-containing species on the surface, we calculate the values of x in $TiO_{2-x}N_x$ as x = atomic % of N/atomic % of Ti, resulting in x value of 0.012 and 0.043 for samples annealed in NH_3 for 1 and 2 h, respectively. Compared with other N-modified TiO_2 materials

dx.doi.org/10.1021/nl2028188 | Nano Lett. 2012, 12, 26−32

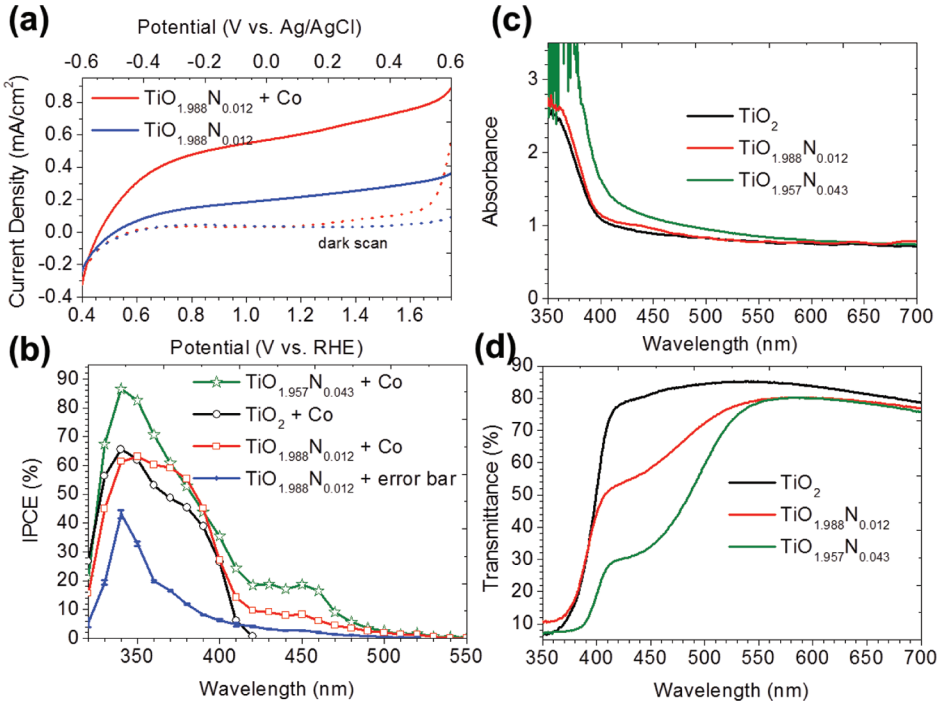

Figure 4. (a) Linear sweep voltammetry of the $TiO_{1.988}N_{0.012}$ sample and the same electrode after cobalt treatment in darkness (dotted lines) and under illumination (solid lines). (b) IPCE spectra of N-modified TiO_2 films at 1.4 V_{RHE}: blue and red curves are the corresponding IPCE spectra of the $TiO_{1.988}N_{0.012}$ photoelectrode in Figure 4a, black curve is the IPCE of unmodified TiO_2 sample after cobalt treatment, and green curve is the IPCE of the $TiO_{1.957}N_{0.043}$ pretreated with cobalt. (c) and (d) UV–vis absorbance and transmittance spectra of unmodified and N-modified TiO_2 nanowire samples, and an as-synthesized sample (black curve) was included as a reference.

synthesized via nitridation of TiO_2 in NH_3, such as a rutile TiO_2 (110) single crystal,[27] anatase powder,[25] anatase films,[28,29] and anatase nanobelts,[22] the substitutional N concentrations in the present films are significantly higher despite lower nitridation temperatures and/or shorter times. We believe that the small feature size of the nanowire arrays allows better nitrogen diffusion into the TiO_2 lattice and that this is likely the key to the enhancement in the N-incorporation level. We performed control tests in which a TiO_2 nanowire sample with a larger average characteristic size (of ~25 nm) prepared by preannealing the as-synthesized TiO_2 nanowire sample in air at 500 °C in 30 min (Figure 3a,2) and a commercial TiO_2 anatase nanoparticle powder with average size of 32 nm (Alfa Aesar; Figure 3a,1) were annealed in NH_3 under the same conditions as our as-synthesized TiO_2 nanowire films (500 °C for 2 h). No N was detected in the XPS spectra, indicating the N uptake is very small, below the detection limit of the XPS instrument (0.1%), thus supporting our hypothesis.

PEC Properties of N-Modified TiO_2 Nanowire Films. Figure 4a shows current–voltage characteristics in dark (blue dotted line) and white (solid blue line) lights for the $TiO_{1.988}N_{0.012}$ film. Compared with unmodified TiO_2 films (Figure 2a), there is a positive shift in the onset potential, E_{on} from 0.2 to 0.5 V_{RHE}. Indeed, the transient photocurrent onset potentials for the two samples are almost the same, at around −0.15 V_{RHE}, indicating that the flat-band potential does not shift with the inclusion of N. In this case,[30] even if the band gap is reduced, the apparent photocurrent onset potential relative to the reference electrode (in a three-electrode cell) should theoretically remain the same. We, therefore, believe that the shift in E_{on} may be due to either a larger banding requirement for separating electrons and holes because of the material's likely possession of poorer charge-transport properties than pure TiO_2 or a slower water oxidation kinetics at the surface of N-modified TiO_2 sample. Moreover, compared to an unmodified sample of the same thickness (1.6 μm), the N-modified sample shows a noticeably lower photocurrent, reaching 0.23 mA/cm^2 at 1.23 V_{RHE}, compared to 0.38 mA/cm^2 for the unmodified TiO_2 nanowire film (Figure 2a). Although most authors report an enhancement in the visible light response for N-modified TiO_2 films, they also observe a significant decrease in quantum yields in the UV region that leads to poor PEC performance under whole spectrum (i.e., white light) illumination.[13,15,25,31] Poor PEC performance has often been explained as being due to the formation of isolated N 2p states above the valence band edge, which act as electron–hole recombination centers. Using time-resolved absorption spectroscopy, Tang et al. reported two distinct photohole populations that are trapped at the N-induced states.[32] They also demonstrated that the lack of water oxidation is due to either rapid electron–hole recombination between charges trapped at the N-incorporation induced states or the reduced oxidative power of the photoholes leading to a lack of thermodynamic driving force. Additionally, Chambers et al. reported that the hole trapping probability at the N-induced states is crystallographically dependent.[33] The hole trapping probability increases if the photogenerated holes diffuse along ⟨110⟩ and ⟨001⟩ directions, and the detrapping probability increases if the holes diffuse along ⟨100⟩ direction. As other authors have suggested, it could be that when incorporating TiO_2 with N, substitutional N 2p states hybridize with O 2p.[4,34] Since the N 2p state has a higher orbital energy than the O 2p state, the orbital hybridization shifts the valence band edge to more negative potentials, thus decreasing the oxidative power of photogenerated holes, which hinders hole transfer rates to oxidizable species on the film surface (H_2O or OH^-). A water

dx.doi.org/10.1021/nl2028188 | Nano Lett. 2012, 12, 26–32

oxidation electrocatalyst, therefore, may be useful in lowering the overpotential for the reaction. In the next section, we present a simple cobalt cocatalyst treatment which improves the PEC performance of our N-modified TiO_2 films.

Water Oxidation Catalyst for N-Modified TiO_2 Nanowire Films. In PEC water splitting, the water oxidation half reaction is normally more challenging than water reduction and is the rate-limiting step since it involves removal of a total of four electrons and four protons from two water molecules to form one oxygen molecule. There have been numerous investigations of water oxidation catalysts for photoanode materials, such as Co-Pi,[11] IrO_x,[9] Pt, Co_3O_4, and IrO_x.[35] However, to our knowledge, there have not been any reports on water oxidation catalysts for N-modified TiO_2 photoanodes. We employed cobalt and silver treatments similar to that mentioned for the unmodified TiO_2 nanowire films in the previous section in which our N-modified TiO_2 films were immersed in either 0.1 M $Co(NO_3)_2$ or 0.05 M $AgNO_3$ solution for 1 min followed by rinsing with a copious amount of water.

Figure 4a shows linear sweep voltammetry of the $TiO_{1.988}N_{0.012}$ photoanode before and after cobalt treatment. After the cobalt treatment, the photocurrent density at 1.23 V_{RHE} increases from 0.23 mA/cm^2 (without cobalt) to 0.61 mA/cm^2 (60% higher than the unmodified TiO_2 sample shown in Figure 2a). Compared to an unmodified sample, the cobalt treatment has a much stronger effect on N-modified TiO_2 samples with around a 2.5-fold improvement in the photocurrent at 1.23 V_{RHE}. Silver treatment on the N-modified TiO_2 film only slightly improves the photocurrent of around 15% at 1.23 V_{RHE} (data not shown), almost the same as for the pristine TiO_2, probably because of the surface passivation effect (Ag is not known as a water oxidation cocatalyst). Therefore, we believe that in this case, the cobalt treatment plays dual roles to passivate surface states, thus increasing hole lifetime, and to form a cobalt-based water oxidation catalyst layer. The main PEC performance enhancement may be primarily from the water oxidation catalytic activity of the cobalt layer. We also performed a long chrono-amperometry measurement which shows no significant change in the photocurrent during 10 min of illumination (data not shown), suggesting good stability of the N-modified TiO_2 nanowire arrays and the cobalt layer. Grätzel et al. proposed a mechanism for the electrocatalysis of water oxidation by cobalt on hematite surfaces which involves Co^{II}/Co^{III} and Co^{III}/Co^{IV} couples.[10] We believe cobalt plays a similar role on N-modified TiO_2 surfaces. Holes photogenerated within the valence band of N-modified TiO_2 have N^{3-} 2p character rather than O^{2-} 2p as in TiO_2, thus having less positive potential which results in slower kinetics for water oxidation. On cobalt modified N-modified TiO_2 surfaces, water oxidation may follow a reaction pathway that does not require the formation of energetic intermediates, such as OH radicals, thus lowering the activation barrier. The photoholes generated within the valence band of pristine TiO_2 have a significant built-in overpotential for water oxidation (~1.6 V),[30] therefore the use of cobalt as a cocatalyst is not necessary.

Photoconversion Efficiency of N-modified TiO_2 nanowire films. IPCE tests were performed in 1 M KOH at 1.4 V_{RHE} to evaluate PEC water oxidation performance of cobalt-treated N-modified TiO_2 films (Figure 4b). The IPCE spectra of N-modified TiO_2 photoanodes have a low-energy threshold at a wavelength of ~520 nm, corresponding to 2.4 eV (IPCE ~1.7% at 520 nm for cobalt-treated $TiO_{1.957}N_{0.043}$), although they weakly responded to photons with wavelengths up to 600 nm (typical calculated IPCEs in the region from 530 to 600 nm were from 0.6 to ~0.05%). For cobalt treated unmodified TiO_2 (black curve), the PEC onset is located at around 420 nm. We note that after the cobalt treatment, the IPCE performance of N-modified TiO_2 films (green and red curves) in the UV region is restored to that of the unmodified samples. This indicates that the low water oxidation quantum yields in the UV region due to N incorporation are likely due to the lower overpotential for water oxidation of photoholes at the N-modified TiO_2 valence band edge. This lower overpotential can apparently be made up by the use of an appropriate water oxidation cocatalyst.

The IPCE spectra fit the absorbance spectra and the transmittance spectra well (Figure 4c,d), which suggests that there are no major relative differences in the oxidative power of the holes photogenerated by UV and visible light photons.[13] The conversion efficiency of visible photons appears to be limited by absorption depth. Moreover, the onset of the IPCE spectra located at ~550 nm confirms that the long tail at longer wavelengths in the UV–vis absorbance spectra for N-modified samples is not solely due to the light scattering of the nanostructure. The plateau in the IPCE spectrum from 420 to 460 nm is well matched up with the plateau in the transmittance spectrum, indicating that the sample absorbs photons within this range with similar efficiency. It is also interesting that the IPCE spectrum in the visible light region (greater than 420 nm) for cobalt treated $TiO_{1.9570}N_{.043}$ (Figure 4b, green curve) is significantly higher than that of cobalt treated $TiO_{1.988}N_{0.012}$ (Figure 4b, red curve). In the visible light region, the IPCE spectrum of the cobalt treated $TiO_{1.957}N_{0.043}$ film plateaus from 420 to 460 nm at values of ~18%, before decaying to ~0.2% at 550 nm. The IPCE spectrum of the cobalt treated $TiO_{1.988}N_{0.012}$ film has a similar shape but with plateau values of ~9% from 420 to 450 nm. It is well established that more N-dopant leads to better visible light absorbance, although unfortunately this has not always lead to better water oxidation performance and photocatalytic activity.[13,22] However, it is clear that by using a water oxidation cocatalyst, the PEC performance of cobalt treated N-modified TiO_2 can be enhanced, resulting in more than a 60% higher full-spectrum photocurrent compared to unmodified TiO_2.

The UV–vis absorbance and transmittance spectra for untreated and Co-treated samples are almost identical, suggesting that the Co-catalyst does not affect the light absorption ability of the materials. Additionally, the IPCE of the Co-treated TiO_2 samples does not show response to wavelengths >420 nm. Compared to pristine TiO_2 nanowire arrays, we observe an additional photoresponse from 420–550 nm, including the plateau from ~420 to ~460 nm in both the IPCE and UV–vis transmittance spectra for all N-modified samples, suggesting that additional N-induced states are present in the range of 0–0.7 eV above the valence band edge of TiO_2 (or 3.0–2.3 eV below the conduction band edge). We believe that the density of these N-induced states is almost constant from 0–0.3 eV above the valence band edge. We, however, did not observe additional electronic states above the valence band edge in valence band XPS or ultraviolet photoemission spectra (Figure S4, Supporting Information) of the N-modified TiO_2 samples.

In summary, we report a hydrothermal synthesis route that allows direct growth of vertically aligned, densely packed, single crystalline rutile TiO_2 nanowire arrays with exceptionally small

dx.doi.org/10.1021/nl2028188 | Nano Lett. 2012, 12, 26–32

feature sizes of ~5 nm and lengths up to 4.4 μm on top of FTO substrates. We also report the synthesis of visible light active N-modified TiO_2 photoanodes via the nitridation of hydrothermally synthesized TiO_2 nanowire arrays in NH_3 at relatively low temperatures. We also demonstrate that utilization of a cobalt cocatalyst can significantly enhance the PEC performance of our N-modified TiO_2 nanowire arrays. With a cobalt water oxidation cocatalyst, the quantum yields of our N-modified TiO_2 samples increase with increasing substitutional nitrogen concentration and are higher than the quantum yields of unmodified TiO_2 samples in both UV and visible light regions.

■ ASSOCIATED CONTENT

Supporting Information

Analytical methods, additional SEM images, and valence band XPS and UPS spectra. This material is available free of charge via the Internet at http://pubs.acs.org.

■ AUTHOR INFORMATION

Corresponding Author

*E-mail: mullins@che.utexas.edu.

■ ACKNOWLEDGMENTS

The authors gratefully acknowledge the Division of Chemical Sciences, Geosciences, and Biosciences, Office of Basic Energy Sciences of the U.S. Department of Energy through grant DE-FG02-09ER16119 for funding this work and the Welch Foundation (C.B.M. for grant F-1436 and A.J.B. for grant F-0021).

■ REFERENCES

(1) Fujishima, A.; Honda, K. *Nature* **1972**, *238* (5358), 37–38.
(2) Linsebigler, A. L.; Lu, G.; Yates, J. T. *Chem. Rev.* **1995**, *95* (3), 735–758.
(3) Chen, X.; Mao, S. S. *Chem. Rev.* **2007**, *107* (7), 2891–2959.
(4) Asahi, R.; Morikawa, T.; Ohwaki, T.; Aoki, K.; Taga, Y. *Science* **2001**, *293* (5528), 269–271.
(5) Park, J. H.; Kim, S.; Bard, A. J. *Nano Lett.* **2005**, *6* (1), 24–28.
(6) Zhu, W.; Qiu, X.; Iancu, V.; Chen, X.-Q.; Pan, H.; Wang, W.; Dimitrijevic, N. M.; Rajh, T.; Meyer, H. M.; Paranthaman, M. P.; Stocks, G. M.; Weitering, H. H.; Gu, B.; Eres, G.; Zhang, Z. *Phys. Rev. Lett.* **2009**, *103* (22), 226401.
(7) Yin, W.-J.; Tang, H.; Wei, S.-H.; Al-Jassim, M. M.; Turner, J.; Yan, Y. *Phys. Rev. B* **2010**, *82* (4), 045106.
(8) Salvador, P. *J. Appl. Phys.* **1984**, *55* (8), 2977–2985.
(9) Abe, R.; Higashi, M.; Domen, K. *J. Am. Chem. Soc.* **2010**, *132* (34), 11828–11829.
(10) Kay, A.; Cesar, I.; Grätzel, M. *J. Am. Chem. Soc.* **2006**, *128* (49), 15714–15721.
(11) Kanan, M. W.; Nocera, D. G. *Science* **2008**, *321* (5892), 1072–1075.
(12) Burda, C.; Lou, Y.; Chen, X.; Samia, A. C. S.; Stout, J.; Gole, J. L. *Nano Lett.* **2003**, 3 (8), 1049–1051.
(13) Beranek, R.; Neumann, B.; Sakthivel, S.; Janczarek, M.; Dittrich, T.; Tributsch, H.; Kisch, H. *Chem. Phys.* **2007**, *339* (1–3), 11–19.
(14) Nakamura, R.; Tanaka, T.; Nakato, Y. *J. Phys. Chem. B* **2004**, *108* (30), 10617–10620.
(15) Torres, G. R.; Lindgren, T.; Lu, J.; Granqvist, C. G.; Lindquist, S. E. J *J. Phys. Chem. B* **2004**, *108* (19), 5995–6003.
(16) Batzill, M.; Morales, E. H.; Diebold, U. *Phys. Rev. Lett.* **2006**, *96* (2), 026103.
(17) Serpone, N. *J. Phys. Chem. B* **2006**, *110* (48), 24287–24293.
(18) Emeline, A. V.; Sheremetyeva, N. V.; Khomchenko, N. V.; Ryabchuk, V. K.; Serpone, N. *J. Phys. Chem. C* **2007**, *111* (30), 11456–11462.
(19) Feng, X.; Shankar, K.; Varghese, O. K.; Paulose, M.; Latempa, T. J.; Grimes, C. A. *Nano Lett.* **2008**, *8* (11), 3781–3786.
(20) Meinan, L.; Hongxia, W.; Cheng, Y.; Geoffrey, W.; John, B. *Appl. Phys. Lett.* **2011**, *98*, 133113.
(21) Shao, F.; Sun, J.; Gao, L.; Yang, S.; Luo, J. *ACS Appl. Mater. Interfaces* **2011**, *3* (6), 2148–2153.
(22) Wang, J.; Tafen, D. N.; Lewis, J. P.; Hong, Z.; Manivannan, A.; Zhi, M.; Li, M.; Wu, N. *J. Am. Chem. Soc.* **2009**, *131* (34), 12290–12297.
(23) Chen, X.; Burda, C. *J. Am. Chem. Soc.* **2008**, *130* (15), 5018–5019.
(24) Fujishima, A.; Zhang, X. T.; Tryk, D. A. *Surf. Sci. Rep.* **2008**, *63* (12), 515–582.
(25) Irie, H.; Watanabe, Y.; Hashimoto, K. *J. Phys. Chem. B* **2003**, *107* (23), 5483–5486.
(26) Takahashi, I.; Payne, D. J.; Palgrave, R. G.; Egdell, R. G. *Chem. Phys. Lett.* **2008**, *454* (4–6), 314–317.
(27) Diwald, O.; Thompson, T. L.; Zubkov, T.; Walck, S. D.; Yates, J. T. *J. Phys. Chem. B* **2004**, *108* (19), 6004–6008.
(28) Miyauchi, M.; Ikezawa, A.; Tobimatsu, H.; Irie, H.; Hashimoto, K. *Phys. Chem. Chem. Phys.* **2004**, *6* (4), 865–870.
(29) Irie, H.; Washizuka, S.; Yoshino, N.; Hashimoto, K. *Chem. Commun.* **2003**, *11*, 1298–1299.
(30) Gai, Y.; Li, J.; Li, S.-S.; Xia, J.-B.; Wei, S.-H. *Phys. Rev. Lett.* **2009**, *102* (3), 036402.
(31) Lindgren, T.; Lu, J.; Hoel, A.; Granqvist, C. G.; Torres, G. R.; Lindquist, S. E. *Sol. Energy Mater. Sol. Cells* **2004**, *84* (1–4), 145–157.
(32) Tang, J.; Cowan, A. J.; Durrant, J. R.; Klug, D. R. *J. Phys. Chem. C* **2011**, *115* (7), 3143–3150.
(33) Ohsawa, T.; Henderson, M. A.; Chambers, S. A. *J. Phys. Chem. C* **2010**, *114* (14), 6595–6601.
(34) Asahi, R.; Taga, Y.; Mannstadt, W.; Freeman, A. J. *Phys. Rev. B* **2000**, *61* (11), 7459.
(35) Ye, H.; Park, H. S.; Bard, A. J. *J. Phys. Chem. C* **2011**, *115* (25), 12464–12470.